Vol. 29 (1998) *ACTA PHYSICA POLONICA B* No 10

TWO-LOOP QCD CORRECTIONS TO HIGGS-PAIR PRODUCTION AT THE LHC*

S. Dawson

Physics Department, Brookhaven National Laboratory
Upton, NY 11973, USA

S. Dittmaier

Theory Division, CERN, CH–1211 Geneva 23, Switzerland

and M. Spira

II. Institut für Theoretische Physik, Universität Hamburg,
Luruper Chaussee 149, D–22761 Hamburg, Germany

(Received July 9, 1998)

The calculation of the next-to-leading order QCD corrections to the production of a neutral Higgs-boson pair is briefly summarized. The dominant production mechanism is gluon fusion via top-quark loops, so that the QCD corrections can be considered, to good approximation, in the limit of a heavy top-quark mass.

PACS numbers: 12.38.Bx

1. Introduction

The search for Higgs bosons and the investigation of their properties will be one of the most important tasks in future high-energy collider experiments. Direct information on the Higgs potential, which reveals the details of the mass-generation mechanism in spontaneously broken gauge theories, can only be obtained by measuring the self-interactions of the found Higgs boson(s), *i.e.* by searching for multiple-Higgs production processes. In this article we briefly summarize the results of Ref. [1] in which we discussed the QCD corrections to the production of neutral Higgs-boson pairs in *pp* collisions at next-to-leading order (NLO) in the framework of both the Standard Model (SM) and its minimal supersymmetric extension (MSSM).

* Presented by S. Dittmaier at the DESY Zeuthen Workshop on Elementary Particle Theory "Loops and Legs in Gauge Theories", Rheinsberg, Germany, April 19-24, 1998.

The most important production mechanism of Higgs-boson pairs in pp collisions is gluon fusion through a heavy-quark loop, *i.e.* a NLO prediction requires a two-loop calculation. The calculational standard for multiloop diagrams is, however, not high enough yet to allow for an exact analytical evaluation of massive two-loop vertex and box diagrams. Fortunately, the structure of the relevant diagrams admits a feasible approximation that is also phenomenologically reasonable. It consists in an asymptotic expansion in a heavy top-quark mass, $m_t \to \infty$, and the neglect of the b-quark mass, $m_b = 0$. Therefore, we have calculated the relative NLO corrections in this limit, but taking into account the known leading-order (LO) cross section [2] exactly. The analogous procedure for single-Higgs production at LHC energies reproduces the exactly known two-loop result within 5% for Higgs-boson masses below the $2m_t$ threshold of the top-quark loops; even for Higgs-boson masses up to 1 TeV the deviation does not exceed 10%. This impressive reliability is due to the dominance of universal soft-gluon effects [3], which do not resolve the detailed structure of the hard-scattering process and are fully included in the approximation. Therefore, we expect that our results for Higgs-pair production are valid at the 10% level, at least for invariant masses of the Higgs-boson pair below $2m_t$.

For the production of Higgs-boson pairs in the MSSM a few more remarks are in order. The neglect of m_b forces us to choose tgβ small, since the b-quark Yukawa coupling is enhanced, and thus non-negligible, for large tgβ. Moreover, we consistently neglect squark-loop contributions, *i.e.* we assume squark masses to be large. The production channels for a scalar and a pseudoscalar Higgs-boson pair, hA and HA, represent an exceptional case, because they receive also non-negligible contributions from the Drell–Yan-like mechanism via $q\bar{q}$ fusion, which are, however, well known at LO and NLO. More details can be found in Ref. [1].

2. Calculational framework

The LO predictions for the gluon-fusion processes $gg \to \phi_1\phi_2$, where $\phi_1\phi_2$ stands for any neutral Higgs-boson pair, via quark loops are known, including the exact dependence on the heavy-quark masses [2]. The following one-loop diagrams contribute:

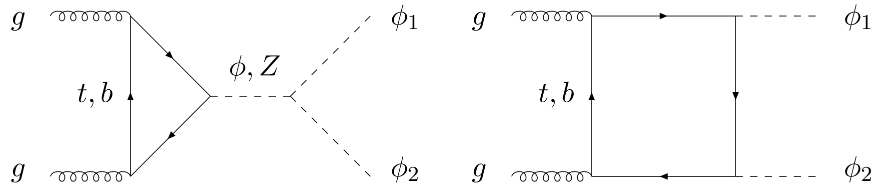

where the Z-boson exchange in the s-channel is only relevant for hA and HA production. At NLO, we get virtual corrections formed by two-loop diagrams, which contain a closed quark loop and one, two or three internal gluons. Moreover, there are real one-loop corrections induced by the parton processes $gg \to \phi_1\phi_2 g$, $gq \to \phi_1\phi_2 q$, and $q\bar{q} \to \phi_1\phi_2 g$. After summing virtual and real corrections, IR divergences drop out; the remaining collinear singularities are absorbed in the parton distributions when calculating the pp cross section.

For the heavy-mass expansion of the diagrams containing the top quark we employ the general algorithm of Ref. [4]. The actual expansion is carried out in the integrand of a diagram, *i.e.* before the momentum-space integration, and relies on dimensional regularization. The general algorithm is easily summarized. Given any Feynman graph Γ with some large internal masses M_i, and denoting the corresponding amplitude and integrand by F_Γ and I_Γ, respectively, the large-mass expansion reads

$$F_\Gamma = \int \left(\prod_l d^n q_l\right) I_\Gamma \ \ \widetilde{\scriptstyle M_i\to\infty}\ \ \sum_\gamma \int \left(\prod_l d^n q_l\right) I_{\Gamma/\gamma}\, \mathcal{T}_{p_i^\gamma, m_i} I_\gamma, \qquad (1)$$

where q_l are the integration momenta. The sum on the r.h.s. runs over all subgraphs γ of Γ that contain all propagators with the heavy masses M_i and that are irreducible with respect to those lines of γ that carry light masses m_i. The integrand of the subgraph γ is denoted by I_γ. The reduced graph Γ/γ results from Γ upon shrinking γ to a point, and the integrand $I_{\Gamma/\gamma}$ is defined such that $I_\Gamma = I_\gamma I_{\Gamma/\gamma}$. The symbol $\mathcal{T}_{p_i^\gamma, m_i}$ represents an operator that replaces the integrand I_γ by its Taylor series in the expansion parameters p_i^γ and m_i, where p_i^γ are the external momenta of the subgraph γ. Therefore, Eq. (1) expresses the original integral F_Γ by a sum over simpler integrals with a finite number of terms in each order M_i^a.

As an illustrating example, we inspect the following box diagram.

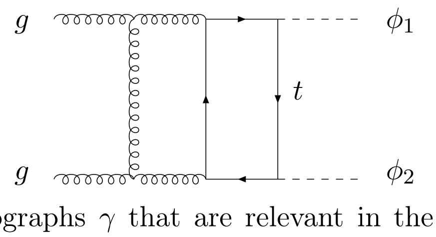

There are two subgraphs γ that are relevant in the expansion (1) of this graph. The first one, $\gamma_{\rm loop}$, consists of all internal lines, the second one, $\gamma_{\rm top}$, consists of the top-quark lines only. The reduced graphs look as follows.

$\Gamma/\gamma_{\rm loop}$:

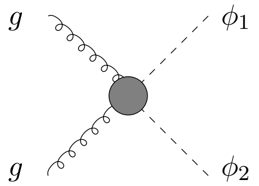

$\Gamma/\gamma_{\rm top}$:

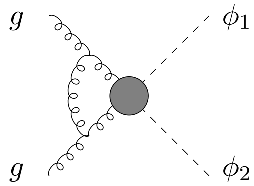

In the case of $\gamma_{\rm loop}$ the Taylor-expansion operator replaces each propagator $P(q-p,m)$ with $m=0,m_t$ by

$$P(q-p,m)=[(q-p)^2-m^2]^{-1}=\sum_{l=0}^{\infty}(q^2-m^2)^{-1-l}(2qp-p^2)^l, \quad (2)$$

where q is a linear combination of the two integration momenta q_1 and q_2, and p consists of external momenta p_i. This replacement leads to two-loop vacuum integrals of the form

$$\int d^n q_1 \int d^n q_2 \, \frac{q_{1,\mu_1}\cdots q_{1,\mu_R}\, q_{2,\nu_1}\cdots q_{2,\nu_S}}{(q_1^2)^{n_1}(q_2^2-m_t^2)^{n_2}[(q_1+q_2)^2-m_t^2]^{n_3}}, \quad (3)$$

the calculation of which is straightforward in n dimensions. For $\gamma_{\rm top}$ the Taylor expansion concerns only the top-quark propagators, and the replacement (2) applies for $m=m_t$ and $q=q_2$, where q_2 is the loop momentum running through the top-quark loop. Note that p now includes all external momenta of the process as well as the loop momentum q_1 running through the internal gluon lines. Thus, the integration over q_2 yields simple one-loop vacuum integrals

$$\int d^n q_2 \, \frac{q_{2,\mu_1}\cdots q_{2,\mu_R}}{(q_2^2-m_t^2)^{n_1}}, \quad (4)$$

while the q_1 integration leads to one-loop integrals of the form

$$\int d^n q_1 \, \frac{q_{1,\mu_1}\cdots q_{1,\mu_R}}{q_1^2(q_1+p_1)^2}, \qquad \int d^n q_1 \, \frac{q_{1,\mu_1}\cdots q_{1,\mu_R}}{q_1^2(q_1+p_1)^2(q_1+p_2)^2}, \quad (5)$$

containing massless propagators and non-vanishing external momenta p_1 and p_2.

It is interesting to realize the close connection of the diagrammatic expansion algorithm described above and the independent approach using a low-energy effective theory. The effective Lagrangian results from integrating out the heavy top quark from the full theory and quantifies the local interactions between light Higgs bosons and gluons at low energies induced by heavy-quark loops. The effective interactions that are relevant in our case are known in LO as well as in NLO and are summarized in Ref. [1]. The effective couplings can be derived from the gluon self-energy upon differentiation, except for the ones that involve an odd number of pseudoscalar

Higgs bosons. The latter are related to the ABJ anomaly. We have also calculated the NLO corrections to $gg \to \phi_1\phi_2$ in the effective-Lagrangian approach. There is a one-to-one correspondence between the sum of all topologically equal reduced graphs Γ/γ in the diagrammatical expansion and the corresponding effective diagram in which γ is identified with the effective coupling. More precisely, the effective couplings enter the NLO corrections in two different ways. Firstly, the NLO parts of the effective interactions contribute in tree-level diagrams like $\Gamma/\gamma_{\rm loop}$. Secondly, the LO parts of the effective couplings contribute in one-loop diagrams like $\Gamma/\gamma_{\rm top}$, which are the only sources of non-local effects.

Although we set $m_b = 0$, there are contributions from b-quark loops in the hA and HA production channels. These contributions are associated with Z-boson exchange and have to be considered separately. The virtual two-loop corrections in the Zgg vertex are fully detemined by gauge invariance, because only a single form factor contributes. The divergence of the Zgg vertex is related by a Ward identity to the coupling of a pseudoscalar field to two gluons, implying that the Zgg vertex correction coincides with the one for single A production, which gets no b-quark contribution for $m_b = 0$. The b-quark loops appearing in the real corrections do not possess a simple form. However, the dominant effects, the ones that are sensitive to soft gluons, are already included by taking into account the Zgg vertex only, leading again to the same correction as for the Agg vertex.

3. Results

The final analytical results for the NLO corrections to the process $pp \to \phi_1\phi_2 + X$ have a rather compact form in the adopted approximation. In this context, the LO cross section $\hat\sigma_{\rm LO}$ of the parton process $gg \to \phi_1\phi_2$ is of central importance:

$$\hat\sigma_{\rm LO}(\hat s = Q^2) = \int d\hat t\, \frac{G_F^2\alpha_s^2(\mu)}{256(2\pi)^3}\left\{|C_\triangle F_\triangle + C_\Box F_\Box|^2 + |C_\Box G_\Box|^2\right\}, \quad (6)$$

where Q is the invariant mass of the Higgs-boson pair, and $\hat s$, $\hat t$, $\hat u$ are the usual Mandelstam variables in the partonic centre-of-mass (CM) system. The functions $C_{\triangle,\Box}$ contain coupling factors and s-channel propagators, and $F_{\triangle,\Box}$ and $G_\Box$ represent the form factors corresponding to the two tensors that are relevant for spin-0 and spin-2 exchange. The explicit expressions of the C's, F's, and G's, including the full fermion-mass dependence for the latter two, are given in Ref. [2]. Here we only give the C's and the asymptotic form of the form factors for the SM:

$$
\begin{aligned}
C_\triangle &= \frac{3M_H^2}{\hat{s}-M_H^2+iM_H\Gamma_H}, \qquad C_\Box = 1, \\
F_\triangle &\to \tfrac{2}{3}, \qquad F_\Box \to -\tfrac{2}{3}, \qquad G_\Box \to 0 \qquad \text{for } m_t\to\infty,\ m_b=0. \qquad (7)
\end{aligned}
$$

Note, however, that the exact form of the form factors is used in the numerical evaluations.

All contributions to the pp cross section $\sigma_{\rm NLO}$,

$$
\sigma_{\rm NLO} = \sigma_{\rm LO} + \Delta\sigma_{\rm virt} + \Delta\sigma_{gg} + \Delta\sigma_{gq} + \Delta\sigma_{q\bar{q}}, \qquad (8)
$$

can be written as a convolution of a correction factor, of $\hat{\sigma}_{\rm LO}$, and of the parton–parton luminosities $d\mathcal{L}^{ij}/d\tau$:

$$
\begin{aligned}
\sigma_{\rm LO} &= \int_{\tau_0}^{1} d\tau\, \frac{d\mathcal{L}^{gg}}{d\tau}\, \hat{\sigma}_{\rm LO}(\tau s), \\
\Delta\sigma_{\rm virt} &= \frac{\alpha_s(\mu)}{\pi}\int_{\tau_0}^{1} d\tau\, \frac{d\mathcal{L}^{gg}}{d\tau}\, \hat{\sigma}_{\rm LO}(\tau s)\, C, \\
\Delta\sigma_{gg} &= \frac{\alpha_s(\mu)}{\pi}\int_{\tau_0}^{1} d\tau\, \frac{d\mathcal{L}^{gg}}{d\tau}\int_{\tau_0/\tau}^{1}\frac{dz}{z}\, \hat{\sigma}_{\rm LO}(z\tau s)\left\{-zP_{gg}(z)\log\frac{M^2}{\tau s}\right. \\
&\quad \left. -\frac{11}{2}(1-z)^3 + 6[1+z^4+(1-z)^4]\left(\frac{\log(1-z)}{1-z}\right)_+\right\}, \\
\Delta\sigma_{gq} &= \frac{\alpha_s(\mu)}{\pi}\int_{\tau_0}^{1} d\tau\sum_{q,\bar{q}}\frac{d\mathcal{L}^{gq}}{d\tau}\int_{\tau_0/\tau}^{1}\frac{dz}{z}\, \hat{\sigma}_{\rm LO}(z\tau s) \\
&\quad \times\left\{-\frac{z}{2}P_{gq}(z)\log\frac{M^2}{\tau s(1-z)^2} + \frac{2}{3}z^2 - (1-z)^2\right\}, \\
\Delta\sigma_{q\bar{q}} &= \frac{\alpha_s(\mu)}{\pi}\int_{\tau_0}^{1} d\tau\sum_{q}\frac{d\mathcal{L}^{q\bar{q}}}{d\tau}\int_{\tau_0/\tau}^{1}\frac{dz}{z}\, \hat{\sigma}_{\rm LO}(z\tau s)\,\frac{32}{27}(1-z)^3, \qquad (9)
\end{aligned}
$$

where $\sqrt{s}$ is the total CM energy in the pp system, and $\sqrt{\tau_0 s} = m_1+m_2$ is the corresponding threshold for the production of two Higgs bosons with masses m_1 and m_2. The renormalization and factorization scales are denoted by μ and M, respectively, and $P_{ij}(z)$ are the Altarelli–Parisi splitting functions. While the form of the real corrections $\Delta\sigma_{gg,gq,q\bar{q}}$ is universal, the virtual correction factors

$$C = \pi^2 + c_1 + \frac{33 - 2N_F}{6} \log \frac{\mu^2}{Q^2} + \Re e \frac{\int d\hat{t} \left\{ c_2 \, C_\Box (C_\triangle F_\triangle + C_\Box F_\Box) + \frac{\hat{t}\hat{u} - m_1^2 m_2^2}{2Q^2} \left(\frac{c_3}{\hat{t}} + \frac{c_4}{\hat{u}} \right) C_\Box^2 G_\Box \right\}}{\int d\hat{t} \, \{ |C_\triangle F_\triangle + C_\Box F_\Box|^2 + |C_\Box G_\Box|^2 \}} \tag{10}$$

do not coincide for all Higgs-boson pairs. The coefficients c_i for the individual final-state Higgs bosons $\phi_1\phi_2$ are given by

$$\begin{array}{lllll} \phi_1\phi_2 = hh, hH, HH: & c_1 = \frac{11}{2}, & c_2 = \frac{4}{9}, & c_3 = \frac{4}{9}, & c_4 = \frac{4}{9}, \\ \phi_1\phi_2 = hA, HA: & c_1 = 6, & c_2 = \frac{2}{3}, & c_3 = -\frac{2}{3}, & c_4 = \frac{2}{3}, \\ \phi_1\phi_2 = AA: & c_1 = \frac{11}{2}, & c_2 = -1, & c_3 = 1, & c_4 = 1. \end{array} \tag{11}$$

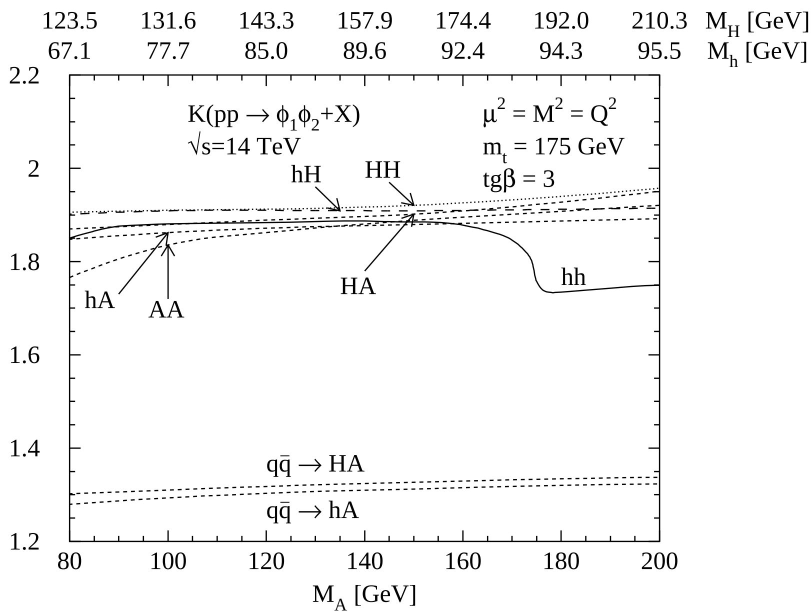

Fig. 1. K factors of the QCD-corrected gluon-fusion and Drell–Yan like cross sections $\sigma(pp \to \phi_1\phi_2 + X)$ at the LHC with CM energy $\sqrt{s} = 14$ TeV.

A detailed numerical study of the QCD corrections described above is presented in Ref. [1] for the SM and the MSSM. Figure 1 summarizes our results on the K factors for Higgs-pair production in the MSSM as functions of the pseudoscalar mass M_A, demonstrating their phenomenological importance at the LHC. The K factor for the SM cross section smoothly varies between 1.9 and 2.0 for a Higgs-boson mass within 80–200 GeV.

S. Dittmaier would like to thank the organizers for the kind invitation and for providing a very pleasant atmosphere during the workshop.

REFERENCES

[1] S. Dawson, S. Dittmaier, M. Spira, hep-ph/9805244.
[2] T. Plehn, M. Spira, P.M. Zerwas, *Nucl. Phys.* **B479**, 46 (1996) and Erratum.
[3] M. Krämer, E. Laenen, M. Spira, *Nucl. Phys.* **B511**, 523 (1998).
[4] V.A. Smirnov, *Phys. Lett.* **B394**, 205 (1997).